Light Metals 2013 *Edited by: Barry Sadler*
TMS (The Minerals, Metals & Materials Society), 2013

MICROHARDNESS, CORROSION BEHAVIOUR AND MICROSTRUCTURES OF DIRECTIONALLY SOLIDIFIED AL-CU ALLOYS

Alicia Ares[1,3] , Carlos M. Rodriguez[1,2]; Claudia M. Mèndez[1]; Carlos E.Schvezov[1,3,4]; Mario R. Rosenberger[1,3];

[1] Materials, Modeling and Metrology Program, Faculty of Sciences, University of Misiones, 1552 Azara Street, 3300 Posadas, Argentina.
[2] Doctoral Fellow of the National Science Research Council of Argentina (CONICET). 1917 Rivadavia Street, 1033, Bs. As., Argentina.
[3] Member of CIC of the CONICET, Argentina. 1917 Rivadavia Street, 1033, Buenos Aires, Argentina. E-mail: aares@fceqyn.unam.edu.ar.
[4] Chairman of the Board of Development and Technological Innovation (CEDIT), 1890 Azara Street, 5th Floor, 3300 Posadas, Argentina.

Keywords: Al-Cu alloys, directional solidification, mechanical properties, corrosion behavior.

Abstract

The aim of this work is to analyze the effect of microstructural parameters (secondary dendritic arm spacings) on the microhardness and corrosion behavior of hypoeutectic Al-Cu alloys. Experimental results include HV microhardness values, corrosion and pitting potential and current density. It was found that high cooling rates during solidification provide finer dendritic spacings, which encourage better mechanical properties. The Vickers microhardness increases as the contents of copper in the alloy increases. The most influencing microstructural variable for corrosion resistance has been found to be the secondary dendrite arm spacing. It has been found that that corrosion resistance decreases with the increasing in secondary spacing until 10wt.% of Cu.

Introduction

A typical cast structure consists of one or both types of grains: columnar or equiaxed. When both are present, the columnar is the first to solidify and then the equiaxed grains are usually formed in the central part of the cast. In such case, the transition is defined as columnar-to-equiaxed transition (CET). A low solidification rate favors the CET phenomenon as well as the addition of nucleant particles [1-7].

Osorio et al. [8] studied the role of macrostructural morphology and grain size in the corrosion resistance of different alloy systems and concluded for Zn-Al alloys that a better corrosion resistance tendency is achieved with coarse macrostructures rather than with fine grains for both Zn and Al.

In previous works, we correlated the effect of several parameters, like thermal and metallurgical ones, with electrochemical parameters on the CET macrostructure in Zn-Al alloys [9]. We were able to observe the susceptibility to corrosion of the alloys with columnar structure by analyzing the values of charge-transfer resistance (R_{ct}) obtained using the Electrochemical Impedance Spectroscopy (EIS) technique.

Another recent research [10] shows that what actually affects the response to corrosion is the way in which aluminum is distributed in the alloy, i.e., which phases are present in the solidified microstructure and how they are distributed, and not the amount of aluminum present in the alloy.

The above results show the strong relation between the solidification process parameters, the resulting structure and the mechanical and corrosion properties of the directionally solidified alloys.

The aim of this work is to analyze the effect of microstructural parameters (secondary dendritic arm spacings) on the microhardness and corrosion behavior of hypoeutectic Al-Cu alloys.

Materials and Methods

The Al-Cu alloys (from 1wt.%Cu to 33.2wt.%Cu) were solidified directionally upwards in an experimental set up consisting of a heating unit, a temperature control system, a temperature data acquisition system, a sample moving system and a heat extraction system. The set up is shown in Figure 1. After solidification the samples were cut in the axial direction, the samples were polished and etched with a solution consisting of 15ml HF, 4.5ml HNO_3, 9ml HCl, 271.5ml H_2O, in the case of the alloys with less than 10%wtCu. A solution of 320ml HCl, 160ml HNO_3, 20ml HF was utilized as etching for alloys with more than 10%wtCu [11-13]. The position of the transition was determined by observation under an optical microscope.

Dendritic spacing measurements were made using the linear interception technique, preferably in regions close to the positions of the thermocouples during directional solidification.

Microhardness measurements were performed at room temperature with a Leitz Durimet ® microhardness tester. Loads between 50 g were used. The measurements were performed under ASTM E 384-89 [13] standard using a pressing time of 15 seconds.

For the electrochemical tests (samples were prepared, which are used as working electrodes, approximately 2 cm long, each of the three zones (columnar, equiaxed and CET) and for each concentration from sections specimens cut longitudinally sanded to # 1200 SiC particle size, washed in distilled water and dried by natural air flow. All the electrochemical tests were conducted in a 300 ml of a 3% NaCl solution at room temperature using an IM6d ZAHNER® electrik potentiostat coupled to a frequency analyzer system, a glass corrosion cell kit with a platinum counter electrode and a sutured calomel reference electrode (SCE). Polarization curves were obtained using a scanning rate in the range of $0{,}002\ V/s \leq v \leq -0{,}250\ V/s$ from open circuit potential until to 0,250 V. Impedance spectrums were registered in the frequency range of $10\text{-}3Hz \leq f \leq 105\ Hz$ in open circuit.

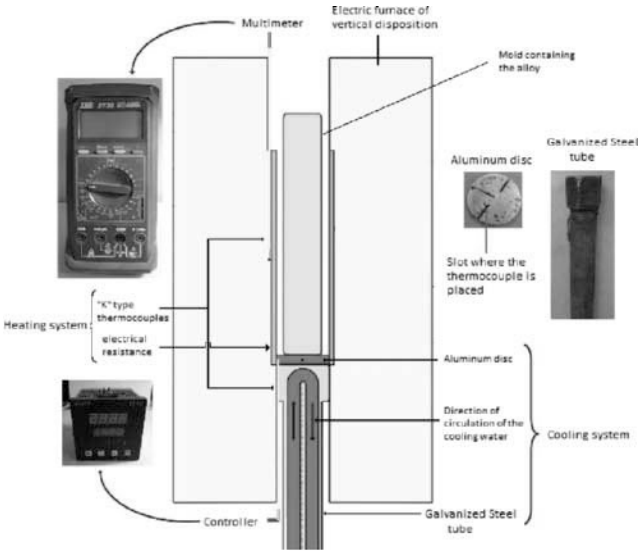

Figure 1. Experimental setup.

Results and Discussion

Columnar-to-Equiaxed Transition (CET)

A number of 15 experiments were performed where the transition from columnar to equiaxed structure was produced. In Figure 2 it is clearly seen that the transition do not occur sharply but in a region of 1cm or more.

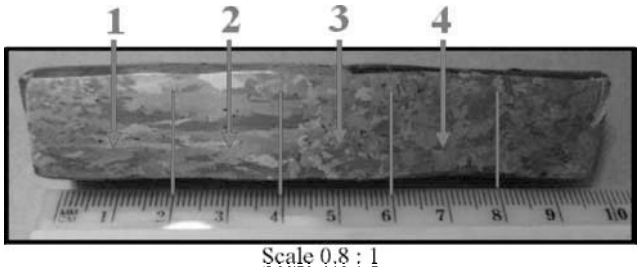

Figure 2. Macrostructure of Al-15%Cu alloy. The red vertical lines are indicates the zones were measured the HV microhardness and dendritic spacings.

Secondary dendritic spacing (λ_2)

Measurements of the secondary dendritic arm spacings include active and inactive branches. In the Figure 3 shows that 1) the structure changes from columnar (base of the sample) to equiaxed (top of the sample) and 2) that it increases with distance from the base.

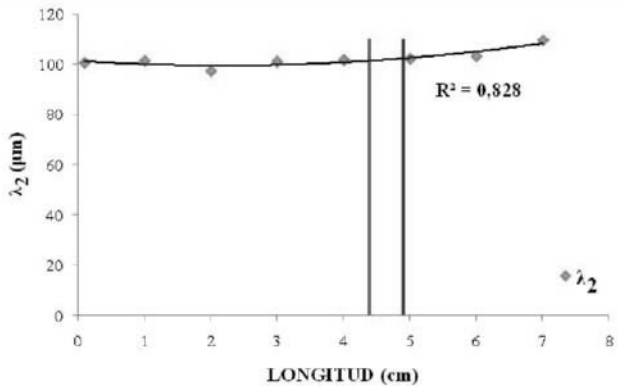

Figure 3. Secondary dendritic arm spacing variation versus the distance from the base of the sample. Al-15wt%Cu alloy.

Vickers Microhardness

To determine an average microhardness, a minimum of 10 measurements were performed in each section of the samples. Figures 4 (a) show experimental results of microhardness variations analyses as a function of sample length, for one alloy, using a load of 50 g_f. It can be seen that Vickers microhardness have greater values in the equiaxed and CET zones of the samples than in the columnar zone.

The results of the microhardness variations analysis as a function of sample width are shown in Figures 4 (b), (c) and (d) for different structures. In all cases we obtain greater microhardness values in sample edges than in the centre of the samples.

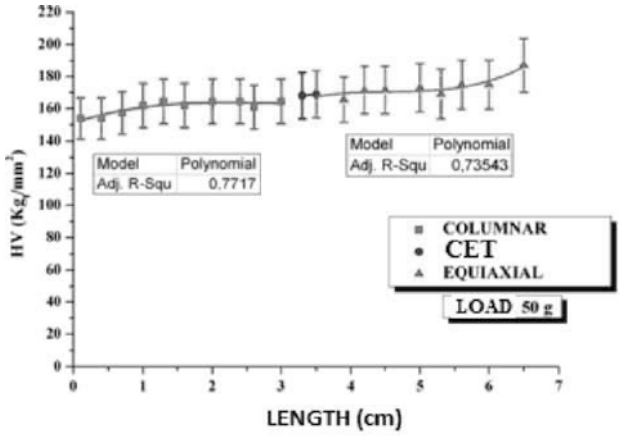

(a)

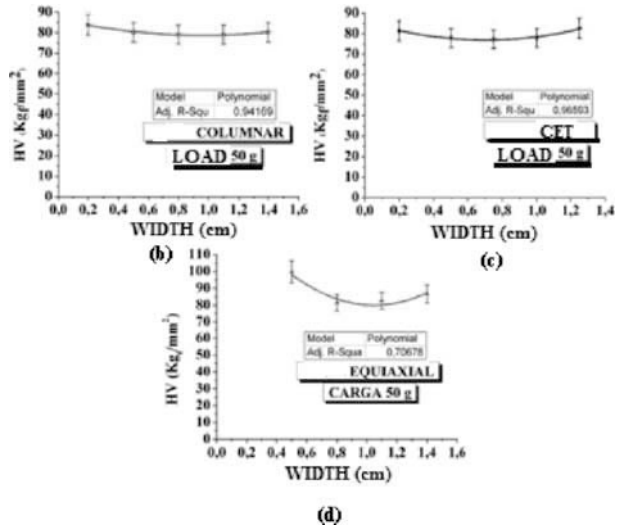

Figure 4. (a) Longitudinal and (b), (c) and (d) Vickers Microhardness in the width of the Al-15wt%Cu alloy sample.

Figure 5 shows the variation in microhardness in function of the concentration of the alloy for the different structures (columnar, equiaxed and CET) from microhardness measurements performed on all samples. It can be appreciated that Vickers microhardness increases as the Copper content in the alloy increases (up to the eutectic composition), and that in all cases, Vickers microhardness is higher in the equiaxed zone. Finally, the Vickers microhardness of the CET zone has values between the values of the columnar and equiaxed zones in all the equiaxed alloy systems.

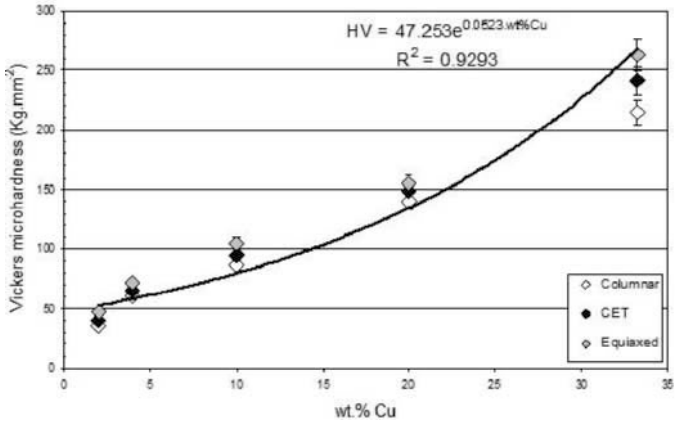

Figure 5. Microhardness versus weight percent of Copper and type of structure.

Figure 6 shows Vickers microhardness as a function of the variation in secondary dendritic spacing. It can be seen that microhardness increases as the λ_2 decreases, i.e., Vickers microhardness increases as the contents of Copper in the alloy increases, and also increases from the columnar to the equiaxed zone.

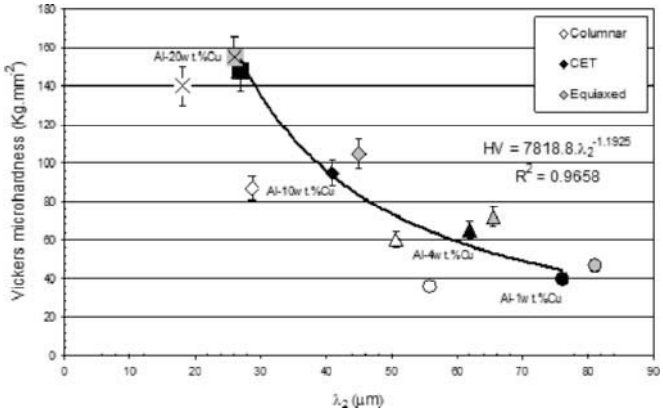

Figure 6. Microhardness versus secondary dendritic arm spacing variation.

Corrosion resistance

The electrochemical response of Al-Cu alloys shows a complex dependence between the concentration of Copper in the alloy and the structure. Figure 7 shows the E / I response of alloys with different amounts of Copper for the equiaxed structure. It is observed that as the concentration of Copper increases the rate of dissolution of the alloy decreases.

While the shape of the voltammograms is similar for each alloy and structure studied this trend with increasing of Copper concentration is not the same for the other two structures (columnar and CET), where although the alloy which increased flows of solution it is the lowest Copper content (Al-2%Cu), this is followed by the alloy with 20% Copper, indicating that there would be a combination strength / structure differently affects the corrosion resistance of each alloy.

Moreover if we compare the current values of the different structures is the columnar which has increased flows of dissolution and equiaxed structure of lower values, regardless of the concentration of the alloy. A similar response was obtained in the transverse specimens in terms of higher current values in the alloy of lower Copper content, but there is no clear correlation between the dissolution process and the Copper content in the alloy.

In all cases, the E / I response of the alloys shows the typical hysteresis indicates the phenomenon of pitting, found that the more susceptible alloys (susceptibility measured as the difference between the potential of pitting and repassivation potential) are the lower Copper content in all its structures. The least susceptible are those containing 10%Copper in its composition, see Figure 8.

Figure 9 shows the Nyquist diagrams obtained for different alloys tested, we could observe that they are virtually just lines depart from the imaginary axis, which indicate that the alloy forms a thick oxide layer. This type of response is repeated for all structures. The impedance results correspond to a simple electrical circuit model that takes into account only one time constant which includes the ability and strength of the surface oxide coating. The values of these parameters are 3 ± 1 μF. cm^{-2} and 9 ± 1 x 10^4 Ω cm^2, typical for oxides formed on Aluminum and its alloys.

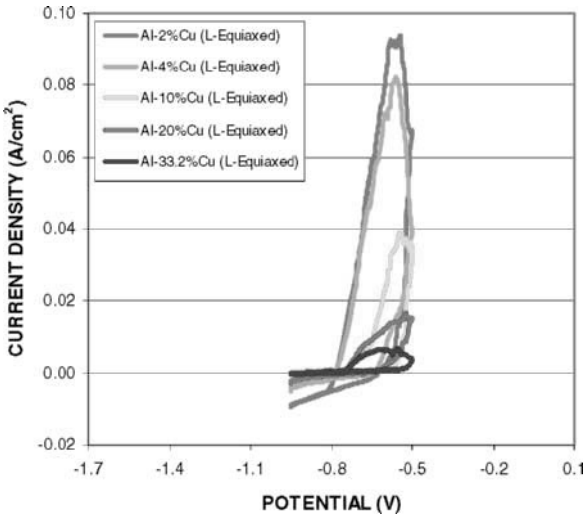

Figure 7. Voltammograms corresponding to Al-Cu alloy samples in the equiaxed zone.

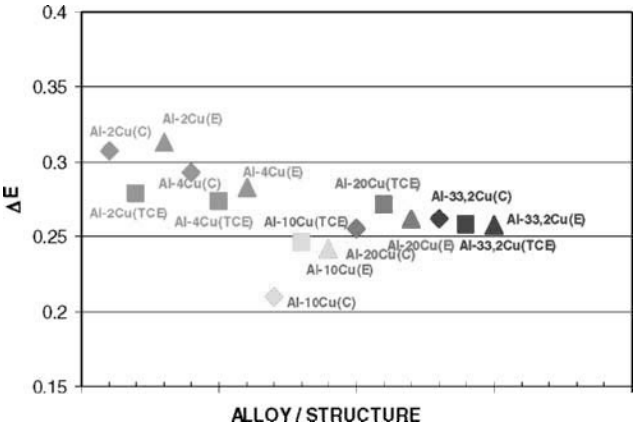

Figure 8. Pitting potential depending on the concentration and structure of the Al-Cu alloy.

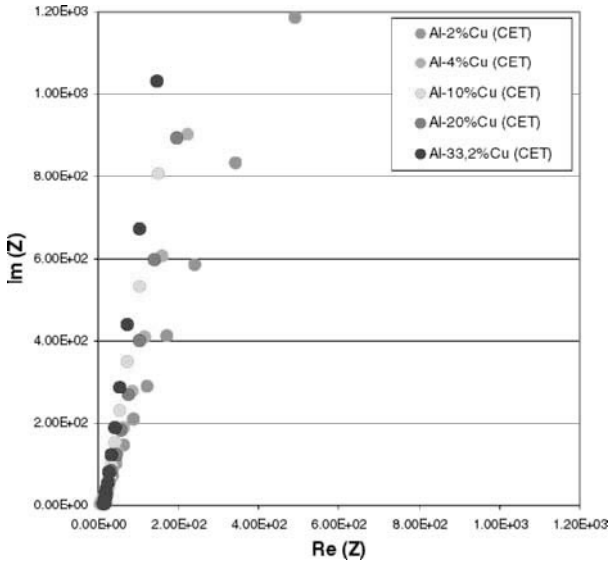

Figure 9. Nyquist diagrams corresponding to Al-Cu alloys in the equiaxed zone.

Analyzing the variation of the secondary dendritic spacing with the concentration of Copper in the alloy (for concentrations between 2% Cu and 20% Cu) and for the three structures (columnar, equiaxed and CET) was obtained that λ_2 decreases with increasing Cu% until 10% and then increases again to the 20% of Cu (similarly to the pitting potential behavior). This was verified for the three types of structures and is consistent with what the literature reported for the same alloy system [1].

In Figure 5 it was found that Al-Cu alloys containing 10% Copper are the less susceptible to corrosion. This behavior is similar to that followed by the λ_2 with increasing Cu concentration.

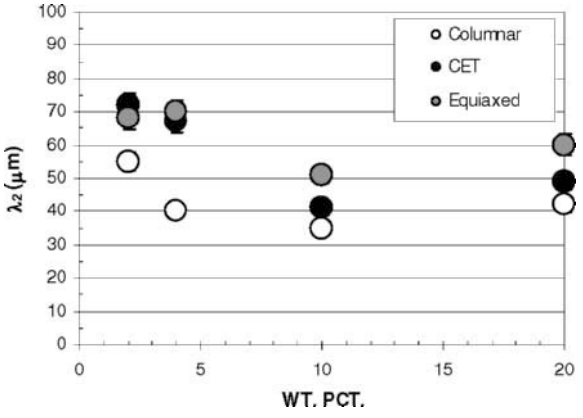

Summary and Conclusions

The main conclusions obtained from the present work are as follow:

1) For the type of alloys studied, i.e Al-1wt%Cu, Al-4.5wt%Cu, Al-15wt%Cu, Al-20wt%Cu and Al-33.2%wtCu, the columnar to equiaxed transition was produced.
2) The Vickers microhardness is greater in the equiaxed zone than in the columnar or columnar to equiaxed transition (CET) and the Vickers microhardness is greater on the edges of the samples than in the centre.
3) The Vickers microhardness increases as the contents of copper in the alloy increases. On the other hand, the Vickers microhardness increases as the λ_2 decreases.
4) As was reported before, the corrosion susceptibility depends on the formation of a thick film of oxide as revealed by the EIS analysis. However, the presence of Copper in their composition makes them susceptible to pitting corrosion.
5) The most influencing microstructural variable for corrosion resistance has been found to be the secondary dendrite arm spacing. It has been found that that corrosion resistance decreases with the increasing in secondary spacing until 10wt.% of Cu (was found that λ_2 have a minimum for a Copper content of about this Copper concentration).

Acknowledgements

This work was supported by PIP 2010-2012 GI 11220090100769 from the Argentinean Research Council (CONICET).

References

1. J.A. Spittle, Columnar to Equiaxed Grain Transition in as Solidified Alloys, Int. Mater. Rev., 51, (2006), 247-269.
2. S.C. Flood, J.D. Hunt, Columnar to Equiaxed Transition, ASM Handbook, ASM. International, Materials Park, OH, 1998.
3. G. Reinhart, N. Mangelinck-Noël, H. Nguyen-Thi, T. Schenk, J. Gastaldi, B. Billia, P. Pino, J. Härtwig, J. Baruchel, Investigation of Columnar-Equiaxed Transition and Equiaxed growth of Aluminium Based Alloys by X-Ray Radiography, Mater. Sci. Eng. A, 413-414, (2005), 384-388.
4. S. McFadden, D.J. Browne, C.A. Gandin, A Comparison of Columnar-to-Equiaxed Transition Prediction Methods Using Simulation of the Growing Columnar Front, Metall. Mater. Trans. A, 40, (2009), 662-672.
5. A.E. Ares, and C.E. Schvezov, Solidification Parameters during the Columnar-to-Equiaxed Transition in Lead-Tin Alloys, Metall. Trans., 31A, (2000), 1611-1625.
6. A.E. Ares, and C.E. Schvezov, Influence of Solidification Thermal Parameters on the Columnar-to-Equiaxed Transition of Al-Zn and Zn-Al Alloys, Metall. Trans., 38 A, (2007), 1485-1499.
7. A. E. Ares, S. F. Gueijman, C. E. Schvezov, An Experimental Investigation of the Columnar-to-Equiaxed Grain Transition in Aluminum-Copper Hypoeutectic and Eutectic Alloys, Journal of Crystal Growth,, 312, (2010), 2154–1170.
8. W.R. Osório, M.E.P. Souza, C.M. Freire, A. Garcia, The Application of Electrochemical Impedance Spectroscopy to Investigate the Effect of As-cast Structures on the Corrosion Resistance of Hypereutectic Zn-Al Alloys, J. New Mat. Electrochem.Systems, 11, (2008), 37-42.
9. A.E. Ares, L.M. Gassa, S.F. Gueijman, C.E. Schvezov, Correlation Between Thermal Parameters, Structures, Dendritic Spacing and Corrosion Behavior of Zn–Al Alloys with Columnar to Equiaxed Transition, J. of Crystal Growth, 310, (2008), 1355-1361.
10. A.E. Ares, L.M. Gassa, Corrosion Susceptibility of Zn–Al Alloys with Different Grains and Dendritic Microstructures in Nacl Solutions, Corros. Sci. , 59, (2012), 290-306.
11. W.J. Moffatt, Handbook of Binary Phase Diagrams, Published by General Electric Company Corporate Research and Development Technology Marketing Operation, New York, (1984), 259, 419, 437, 391.
12. G. Kehl, Fundamentos de la Práctica Metalográfica, Editorial Aguilar, Madrid (1963).
13. H. E. Boyer and T. L.Gall, Metals Handbook, Desk Edition. American Society for Metals, (1990) 35-18. 35-19.